



# Spatial Transcriptomics in Inflammatory Skin Diseases Using GeoMx Digital Spatial Profiling: A Practical Guide for Applications in Dermatology

Christina Cho<sup>1</sup>, Nazgol-Sadat Haddadi<sup>2</sup>, Michal Kidacki<sup>3</sup>, Gavitt A. Woodard<sup>4</sup>, Saeed Shakiba<sup>2</sup>, Ümmügülsüm Yıldız-Altay<sup>2</sup>, Jillian M. Richmond<sup>2</sup> and Matthew D. Vesely<sup>3</sup>

The spatial organization of the skin is critical for its function. In particular, the skin immune microenvironment is arranged spatially and temporally, such that imbalances in the immune milieu are indicative of disease. Spatial transcriptomic platforms are helping to provide additional insights into aberrant inflammation in tissues that are not captured by tissue processing required for single-cell RNA sequencing. In this paper, we discuss a technical and user experience overview of NanoString's GeoMx Digital Spatial Profiler to perform in-depth spatial analysis of the transcriptome in inflammatory skin diseases. Our objective is to provide potential pitfalls and methods to optimize RNA capture that are not readily available in the manufacturer's guidelines. We use concrete examples from our experiments to demonstrate these strategies in inflammatory skin diseases, including psoriasis, lichen planus, and discoid lupus erythematosus. Overall, we hope to illustrate the potential of digital spatial profiling to dissect skin disease pathogenesis in a spatially resolved manner and provide a framework for other skin biology investigators using digital spatial profiling.

**Keywords:** Cutaneous lupus, Digital spatial profiling, Lichen planus, Psoriasis, Spatial transcriptomics

*Journal of Investigative Dermatology* (2025) 5, 1–13; doi:10.1016/j.xjidi.2024.100317

## INTRODUCTION

The skin is a highly organized, immunologically complex organ that maintains tissue homeostasis and serves as the first line of defense against invading pathogens. Immune cells are spatially and temporally organized, with specific cell types residing in designated layers. Disruption of this organization is indicative of injury or chronic disease. Inflammatory skin diseases are characterized by imbalances in the skin's immune microenvironment; however, the molecular mechanisms driving these imbalances are not well-defined. Although traditional histology can help visualize patterns of inflammation and provide insight into disease pathogenesis

and diagnosis, it is limited in its ability to identify the cellular and molecular drivers of the dysregulation. Improved understanding of the direct cell-to-cell interactions and heterogeneity of the skin immune microenvironment that underly inflammatory skin diseases is now available using spatial biology technologies.

Newer methods such as single-cell RNA sequencing (scRNA-seq) have provided critical insights into disease pathogenesis of inflammatory skin diseases such as cutaneous lupus (Billi et al, 2022) and lichen planus (LP) (Hwang et al, 2024<sup>1</sup>). Nevertheless, scRNA-seq lacks spatial information and often requires aggressive processing of samples, which results in cell death, skewing analysis to only a fraction or subset of cells within the tissue. In situ transcriptomics maintains the critical tissue architecture and delineates critical communication pathways between pathogenic cells (Schäbitz et al, 2022; Thrane et al, 2023). Low-plex histological methods such as immunofluorescence (IF) and FISH restrict analysis to a limited number of preknown targets (Langer-Safer et al, 1982; Rudkin and Stollar, 1977). Laser-capture microdissection was pioneered to examine specific pieces of tissue at higher-plex profiling through physical removal of tissue and subsequent bulk sequencing (Emmert-Buck et al, 1996; Meier-Ruge et al, 1976). To overcome these limitations, recent technological advances have allowed for the combination of in situ transcriptomic (Houser et al, 2023; Piñeiro et al, 2022) or proteomic (Veenstra et al,

<sup>1</sup>Department of Immunobiology, Yale School of Medicine, New Haven, Connecticut, USA; <sup>2</sup>Department of Dermatology, University of Massachusetts Medical School, Worcester, Massachusetts, USA; <sup>3</sup>Department of Dermatology, Yale School of Medicine, New Haven, Connecticut, USA; and <sup>4</sup>Department of Surgery, Yale School of Medicine, New Haven, Connecticut, USA

Correspondence: Matthew D. Vesely, Department of Dermatology, Yale School of Medicine, 333 Cedar Street, PO Box 208059, New Haven, Connecticut 06520, USA. E-mail: [matthew.vesely@yale.edu](mailto:matthew.vesely@yale.edu)

Abbreviations: AOI, area of illumination; CTA, Cancer Transcriptome Atlas; DCC, digital count conversion; DEG, differentially expressed gene; DLE, discoid lupus erythematosus; DSP, digital spatial profiling; FDR, false discovery rate; FFPE, formalin-fixed, paraffin-embedded; IF, immunofluorescence; IHC, immunohistochemistry; ISH, in situ hybridization; LMM, linear mixed model; LOQ, limit of quantitation; LP, lichen planus; NGS, next-generation sequencing; PanCK, pan-cytokeratin; QC, quality control; ROI, region of interest; scRNAseq, single-cell RNA sequencing; TMA, tissue microarray; WTA, Whole Transcriptome Atlas

Received 23 September 2023; revised 5 July 2024; accepted 29 August 2024

Cite this article as: *JID Innovations* 2024.100317

<sup>1</sup> Hwang A, Kechter J, Do T, Hughes A, Zhang N, Li X, et al. Oral baricitinib in the treatment of cutaneous Lichen Planus. medRxiv 2024. medRxiv, <https://www.medrxiv.org/content/10.1101/2024.01.09.24300946v1.full.pdf>; 2024 (accessed February 13, 2024).

2021) profiling and are promising tools to decipher cellular connections within intact tissues.

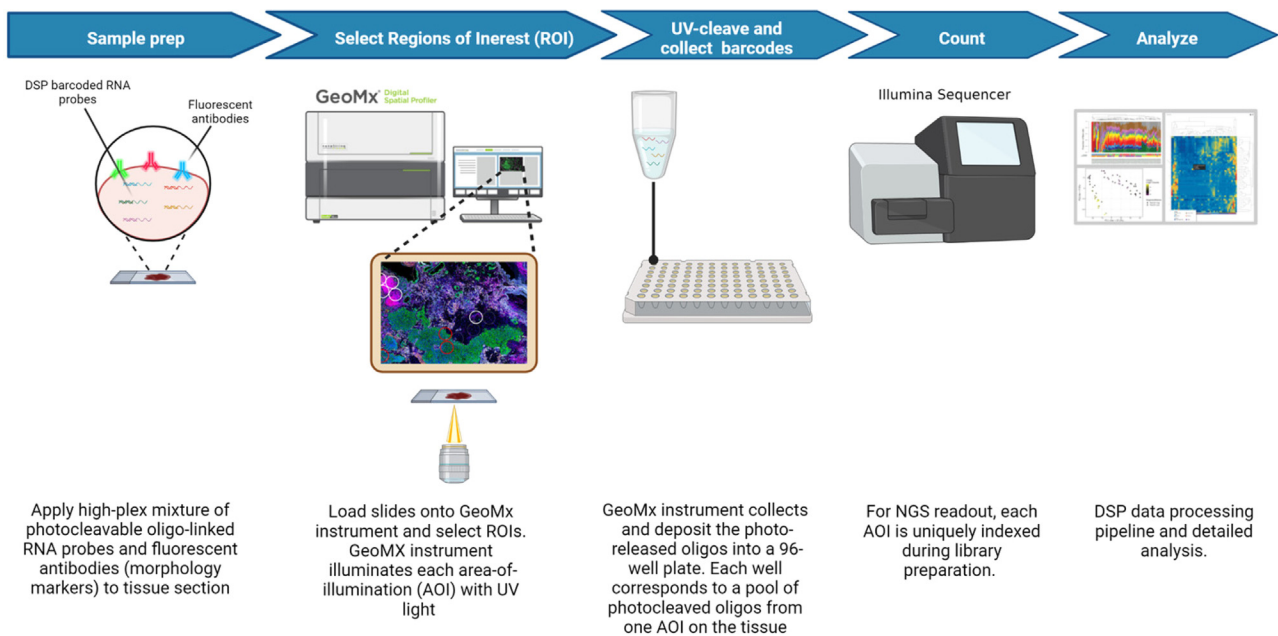
Multiple spatial transcriptomic platforms exist. The 2 most used are Visium by 10x Genomics and GeoMx Digital Spatial Profiler by NanoString. In this paper, we discuss the technical and user experience of GeoMx Digital Spatial Profiler in studying inflammatory skin diseases. Our intention is not to provide a summary of the manufacturer's guidelines but rather a user's perspective on best practices and user-friendly approaches found outside the protocols. GeoMx Digital Spatial Profiler utilizes an optical region of interest (ROI) selection to profile proteins or RNAs on fresh-frozen or formalin-fixed, paraffin-embedded (FFPE) samples with spatial resolution (Merritt et al, 2020). Digital spatial profiling (DSP) has been used for spatial transcriptomic profiling of cancers, including dermatological malignancies, melanoma (Cabrita et al, 2020; Gartrell-Corrado et al, 2020; Helmink et al, 2020; Kiuru et al, 2022; Rozeman et al, 2020; Scatena et al, 2021; Toki et al, 2019; Van Herck et al, 2021; Vathiotis et al, 2021), and cutaneous squamous cell carcinoma (Vesely et al, 2022). Beyond skin cancers, DSP was used on diabetic foot ulcers where skin disaggregation presents technical challenges (Theocharidis et al, 2022). DSP has also been used to study inflammatory skin disease, including psoriasis (Whitley et al, 2022) and hidradenitis (Macchiarella et al, 2023). Therefore, DSP is emerging as a promising tool to spatially interrogate inflammation within skin. In this article, we describe the workflow and technical challenges of DSP transcriptomics profiling of the skin across inflammatory skin diseases, using psoriasis, LP, morphea, and discoid lupus erythematosus (DLE) as concrete examples of potential pitfalls, tips to avoid RNA degradation, and data analysis tools.

## METHODS AND DESCRIPTION

GeoMx Digital Spatial Profiler merges multiplex IF and in situ hybridization (ISH) with digital optical barcoding and subsequent next-generation sequencing (NGS) to perform protein and transcriptomic profiling on intact tissues (Merritt et al, 2020) (Figure 1). Both frozen and FFPE tissues are compatible with this platform; however, for this review, we only discuss best practices when analyzing FFPE samples for transcriptomic profiling. For best practices in profiling proteins using DSP, we refer the reader to an excellent perspective (Van and Blank, 2019). In this paper, we focus on using RNA probes coupled to photocleavable oligonucleotide tags for high-plex transcriptomic analysis in inflammatory skin disease tissues within user-defined ROIs.

### Technical overview of the DSP Platform

The main steps included in the workflow are tissue preparation with immunofluorescent antibodies known as morphology markers and with RNA probes in ISH; ROI selection followed by segmentation and area of illumination (AOI) selection; oligo collection; hybridization, library preparation, and NGS sequencing; and data analysis (Figure 1). The entire workflow from sample preparation to data collection is performed in a stepwise manner that requires a minimum of 5 days. On day 1, biological targets within an FFPE sample are hybridized with UV-cleavable RNA probes. On day 2, cell types of interest are stained with fluorescent antibodies to identify morphology markers, and slides are loaded onto the GeoMx Digital Spatial Profiler instrument, where they are scanned and imaged. Using the morphology markers as a guide, ROIs are selected, and UV-cleaved oligos from those ROIs are collected into a 96-well collection plate. On day 3, the oligos are transferred to a PCR plate for library preparation and sequencing. The PCR products are pooled, purified, and sequenced on an Illumina NGS instrument. On



**Figure 1. NanoString GeoMx Digital Spatial Profiler workflow overview.** Fresh-frozen or FFPE tissues are processed through standard ISH and IHC procedures and costained with photocleavable oligo-linked probes and fluorescent antibodies (morphology markers). Stained slides are loaded onto the GeoMx instrument on which users can define ROIs and AOIs. UV light is shone over the ROIs/AOIs, releasing indexing oligonucleotides that are collected into 96-well plates. These oligonucleotides are then submitted for next-generation sequencing (Illumina) followed by standard library preparation. AOI, area of illumination; FFPE, formalin-fixed, paraffin-embedded; IHC, immunohistochemistry; ISH, in situ hybridization; ROI, region of interest.

day 4, the FASTQ-sequencing files are converted into digital count conversion (DCC) files using Nanostring's GeoMx NGS Pipeline software. The DCC files are then uploaded onto the GeoMx Digital Spatial Profiler Data Analysis Suite for quality control (QC) checks and analysis. Although library preparation and NGS could be performed in 2 days, it will take longer when sending to a sequencing center. In our experience, data are received in the form of converted DCC files 2–4 weeks after oligo collection and submission to sequencing core for library preparation and sequencing. Data analysis is always variable, and although the initial data analysis performed on the GeoMx instrument can be achieved in a couple of days, subsequent analysis for publications may take weeks to months depending on bioinformatic needs.

In the following sections, we review each procedural step, focusing on best practices, potential pitfalls, and methods of troubleshooting. In addition, we discuss the types of biological questions that can be addressed by the GeoMx Digital Spatial Profiler and the procedural factors to consider when addressing those questions.

### Sample preparation for GeoMx Digital Spatial Profiler

**Sample preparation: tissue quality and antibody validation.** The first step for all GeoMx Digital Spatial Profiler experiments is sample preparation (Box 1). For our studies, we have used FFPE, but frozen sections may be used. The first factor to consider is the quality of the tissue, which includes the age of the tissue block and how recently the block was sectioned for the experiment. Nanostring recommends using tissue blocks that are aged <10 years. Tissues stored for longer periods of time may have reduced antigenicity and increased RNA degradation, which produces inconsistent and unreliable results. A previous study evaluating the role of tissue block age on RNA ISH signal demonstrated that detection significantly decreases with increasing block age (Baena-Del Valle et al, 2017). When using archival clinical tissues whose age may exceed 10 years, we recommend testing the quality of RNA by performing RNAscope on a serial section. For our studies, we have restricted samples to no more than the age of 3–5 years to optimize RNA capture and sequencing.

Tissues are then sectioned and mounted onto standard microscope slides. For best results, tissues sections that are <2 weeks prior to performing the experiment should be because the longer tissues are exposed to the environment, the quality of RNA declines. Nanostring recommends that slides be used within 3 months of sectioning; however, we obtained the best results—for morphology

marker staining and sequencing—when samples were prepared within 48 hours of sectioning. If tissue blocks are difficult to obtain and slides must be cut in advance, we recommend double paraffin dipping freshly cut slides and storing in  $-80^{\circ}\text{C}$  to reduce tissue oxidation, resulting in RNA degradation and poor antigen retrieval (Baena-Del Valle et al, 2017). Tissues should be sectioned with 4–6-mm thickness and not larger than the scanning area of 35.3 by 14.4 mm. The antigen retrieval and staining steps have been optimized for 5-mm-thick sections; thus, alterations in tissue thickness would require corresponding adjustments in the tissue preparation protocol. Any tissue outside of the scanning area will not be imaged and may interfere with tissue detection by the optical system. For all our studies, we used 5-mm-thick sections.

Tissue staining and probe hybridization for DSP resemble the procedures for IF and ISH, with 1 major distinction. After deparaffinization, there are 2 antigen retrieval steps instead of a single antigen retrieval step commonly used for standard immunohistochemistry (IHC)/ISH procedures. First, tissues are incubated in Tris-EDTA at pH 9.0 at  $99^{\circ}\text{C}$  for 15–20 minutes. Second, slides are incubated with Proteinase K for 15 minutes at  $37^{\circ}\text{C}$ . This 2-step antigen retrieval protocol with sequential digestion process has very important implications for antibody validation. The addition of the second Proteinase K step can damage certain antigens and epitopes for some antibody clones; thus, it is important to test each antibody morphology marker under these experimental conditions prior to running a complete experiment because not all antibodies compatible with standard IF and IHC protocols will be compatible with the DSP protocol. Antibodies against proteins with abundant expression, such as pan-cytokeratin (PanCK) and CD45, reliably stain various types of tissues and generally do not require validation. Conversely, antibodies against less abundant molecules may require optimization. However, our initial attempts to use CD3 as a morphology marker to profile T cells in the skin failed using a well-validated antibody in IF. For example, anti-CD3e clone C3e/1308 did not stain as well as clone CD3-12 for visualization of T cells under DSP conditions. Therefore, we recommend running a test experiment where you perform all the staining, minus the hybridization of the probes, and scan the tissues on the GeoMx instrument to ensure that all the morphology markers and DNA staining allow you to adequately visualize the tissue. The visualization of the tissue with your markers of interest is how you will select areas for transcriptomic profiling.

After appropriate anti-CD3e antibody validation, we stained 3 samples from LP, DLE, and psoriasis (Table 1) with morphological markers CD3e, CD8a, and PanCK to identify ROIs for subsequent analysis (Figure 2). For each sample, 3 ROIs were selected on the basis of CD3/CD8 staining and a single ROI within the PanCK+ epidermis, where each ROI was a geometric circle measuring 300  $\mu\text{m}$  in diameter. More detailed discussion of ROI selection, tissue segmentation, and analysis is presented below. Visualization of the tissue allows you to select specific areas in distinct spatial locations. For example, clusters of T cells may be selected in the superficial, mid, or deep dermis as well as inflammation in contact with epidermis (Figure 2).

**Sample preparation: selection of probes.** On day 1 of sample preparation, oligo-linked RNA probes are hybridized to the tissues. NanoString provides curated panels of RNA probes and antibodies called the GeoMx RNA and Protein Assays, respectively. There are 3 GeoMx RNA Assays for human samples: the Whole Transcriptome Atlas (WTA), the Cancer Transcriptome Atlas (CTA), and the Immune

#### Box 1. Special considerations for sample preparation

- Use tissues that are aged <10 years, preferably aged <3 years.
- Use slides within 3 months of sectioning, preferably within 2 weeks.
- Double paraffin dip and store unstained slides in  $-20^{\circ}\text{C}$  if using slides >3 months since tissue sectioning.
- Validate antibodies to ensure compatibility with digital spatial profiling workflow.
- Choose appropriate RNA probes for biological question.



**Table 1. Patient Characteristics**

Sample Name	Sex	Age (y)	Location	Treatment at Time of Biopsy	ROIs
CTA panel					
DLE #1	F	45	Cheek	None	1–4
DLE #2	M	53	Nose	None	5–8
DLE #3	F	40	Cheek	None	9–12
LP #1	M	66	Chest	None	1–4
LP #2	F	62	Back	None	5–8
LP #3	M	57	Wrist	None	9–12
PsO #1	F	54	Elbow	None	1–4
PsO #2	M	44	Thigh	None	5–8
PsO #3	F	50	Back	None	9–12
Control #1	F	28	Neck	—	1–4
Control #2	M	52	Back	—	5–8
Control #3	M	33	Back	—	9–12

Abbreviations: CTA, Cancer Transcriptome Atlas; DLE, discoid lupus erythematosus; F, female; LP, lichen planus; M, male; PsO, psoriasis; ROI, region of interest.

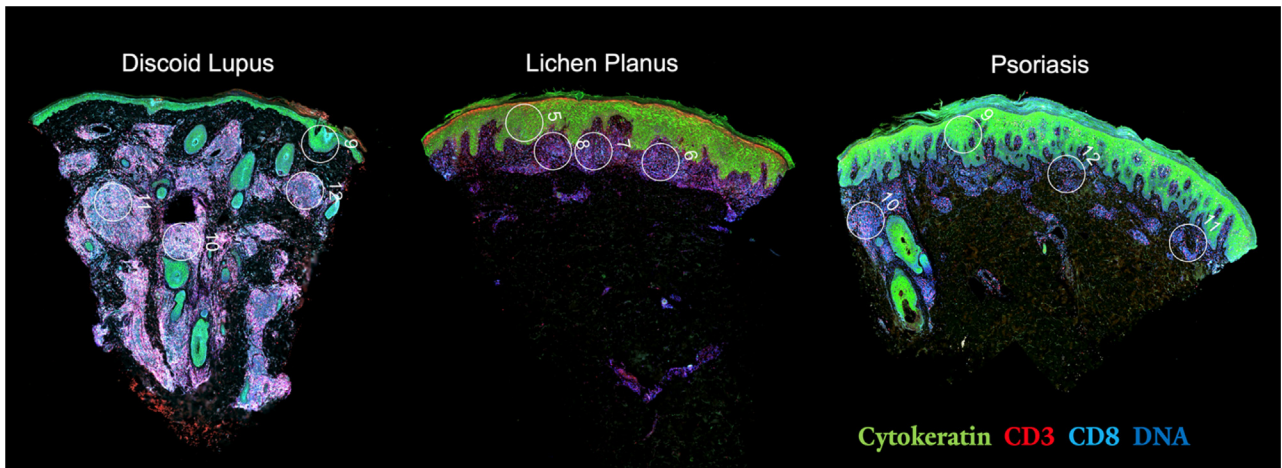
Pathways Panel. The WTA and CTA enable high-plex data analysis using an NGS readout. The WTA covers 18,000 protein-coding genes, whereas the CTA covers 1825 RNA targets related to tumor biology, the tumor microenvironment, and the immune response. The Immune Pathways Panel is a smaller panel of 84 targets plus controls designed for targeted analysis of the tumor, tumor microenvironment, and tumor immune status with customizable 10 additional targets of interest for a total of 96 targets with controls. The readout from the Immune Pathways Panel is compatible with the NanoString nCounter Platform, which does not require amplification, library preparation, or NGS. Whereas these high-plex panels are ideal for discovery-based studies that aim to identify novel molecules that could have biological activity, the lower-plex panel are suitable for more focused studies that aim to understand the function and distribution of known molecules. We will show examples of the data output from using the CTA assay on LP, DLE, and psoriasis tissues in the data analysis section below. The use of histology and morphology markers to guide ROI selection is unique to the DSP

platform with options for marker-specific guided analysis of tissues. Once an ROI is selected, it can be further sectioned into distinct marker-defined areas within an ROI. This type of sectioning is called segmentation, and it enables the separate profiling of specific biological compartments, increasing the probability of capturing rare events commonly missed by bulk sequencing.

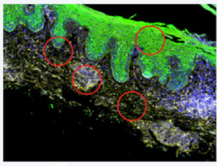

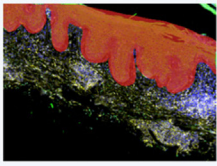

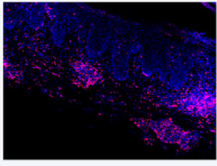
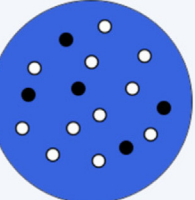
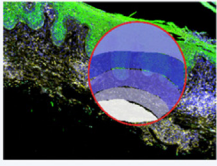
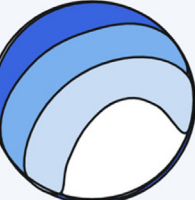
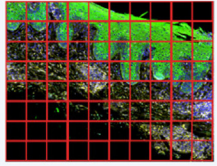
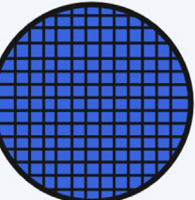
**Selecting ROIs and choosing the appropriate segmentation of tissues**

A unique feature of DSP is its UV masking technology that allows users to study biological compartments within a tissue. Micromirrors within the instrument shine UV light onto areas selected for masking to precisely release indexing oligos. These areas of illumination (AOIs) can be selected using one or a combination of various segmentation profiling tools. There are 5 profiling tools on the DSP: geometric, gridded, gradient, segmentation, and cell-type specific (Figure 3). In this section, we describe each tool and how it can be used to address specific questions for inflammatory skin diseases.

**Geometric ROIs.** Geometric profiling involves the drawing of standardized geometric shapes or custom polygons in various locations of a sample. This strategy is best for profiling large tissue areas or to measure the heterogeneity of the tissue at different sites (Figures 2 and 4). Importantly, geometric profiling can be combined with segmentation, cell-type specific (Figure 5), and gradient profiling. In this section, we show an example of geometric profiling to compare the transcriptomic profile of T lymphocytes and keratinocytes for DLE, LP, and psoriasis. Samples of DLE, LP, and psoriasis were stained with IF antibodies specific for PanCK, CD3e, and CD8 and then counterstained with nuclear dye SYTO (Figure 2). For each sample, 3 ROIs were selected on the basis of CD3+/CD8+ high regions and a single ROI within the PanCK+ epidermis, where each ROI was a geometric circle measuring 300 μm in diameter. For geometric ROIs, the range can be 10–600 μm; however, each ROI must contain at least 20 cells for reliable quantification of transcripts. In our studies, we found that ROIs with <100 cells resulted in poor quantification of transcripts; thus, we recommend drawing an ROI that captures at least 100 cells. Furthermore, during QC, some ROIs may be excluded owing to poor RNA capture that is most likely due to too few cells sampled. Recently, we performed an experiment comparing CD45+



**Figure 2. Visualization of T cells using CD3 and CD8 as morphology markers for ROI selection.** Representative images of discoid lupus, lichen planus, and psoriasis after scanning image in GeoMx DSP instrument. Tissues were stained with pan-cytokeratin (green), CD3e (red), CD8a (cyan), and Syto83 (DNA, blue) for visualization and ROI selection. Each ROI is a geometric circle measuring 300 μm in diameter. DSP, digital spatial profiling; ROI, region of interest.

	Viewing Area	Masking	Objective	Example
<b>Geometric Profiling</b>			Assess tissue heterogeneity and profile standardized geometric shapes across distinct tissue regions	Select distinct adnexal structures that express cytokeratin (e.g. hair follicle vs. sweat glands)
<b>Segmentation</b>			Use morphology markers to identify and profile distinct biological compartments within an ROI	Select epidermis using cytokeratin as the morphology marker
<b>Cell Type Specific</b>			Use Cell type-specific morphology markers to guide profiling to determine function of distinct cell populations	Select CD3 positive cells within the skin microenvironment
<b>Contour</b>			Define a boundary and evaluate how the microenvironment changes on either side (i.e. gradients)	Superficial versus deep
<b>Gridded</b>			Use deep mapping of a specific tissue region to uncover novel targets	Create a grid across entire tissue section for spatial distribution of genes or proteins

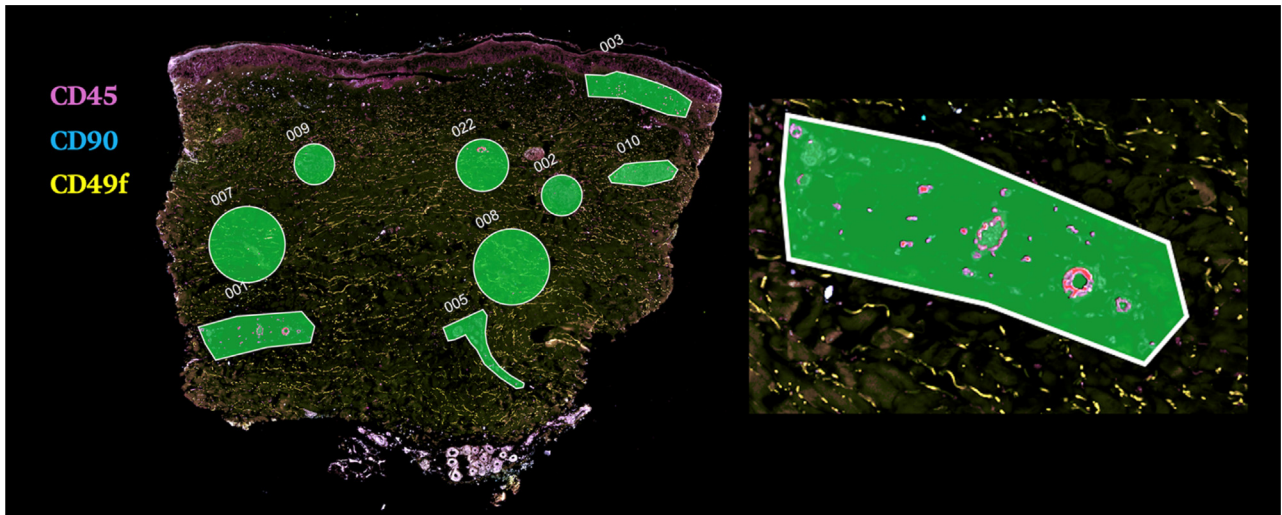
**Figure 3. Distinct approaches to select ROIs for in situ profiling.** There are 5 modalities of ROI selection, including geometric, segmentation, cell-type specific, contour, and gridded. An example of the same psoriasis tissue image used for demonstration is provided. ROI. region of interest.

cells in DLE and LP with those in normal skin. Many ROIs in normal skin failed to capture RNA from enough cells to be reliable after filtering of genes on the basis of limit of quantification metrics and data normalization. This is likely due to the sparse number of CD45+ immune cells in our normal skin specimens. Lack of reliable data can also occur in inflammatory skin diseases if the cells are not clustered close together for profiling. For example, we attempted to performed WTA assay on morphea tissue with multiple spatially distributed geometric ROIs (Figure 4). Ultimately, these ROIs failed QC, and no data analysis was possible owing to low cell numbers in each ROI. This may be due to the fibrosis in morphea and difficulty in capturing nucleated cells. During QC, the GeoMx software performs a technical

background check to ensure the minimum detection of at least 20 estimated nuclei and 1000 transcript reads. Without specific morphology markers to highlight fibroblasts, it may be difficult to detect elongated and spindle-shaped cells. In this case, we used CD45, CD49f, and CD90 select for different fibroblast population (CD45–CD49f+ and CD45–CD90+), but not enough cells were captured in this approach. Therefore, it is critical to choose appropriate morphology markers for visualization and ensure areas of high cellularity when selecting ROI location and profiling tools.

**Gridded ROIs.** Gridded profiling allows for unbiased, deep mapping of a specific tissue region. In gridded profiling, the sample is



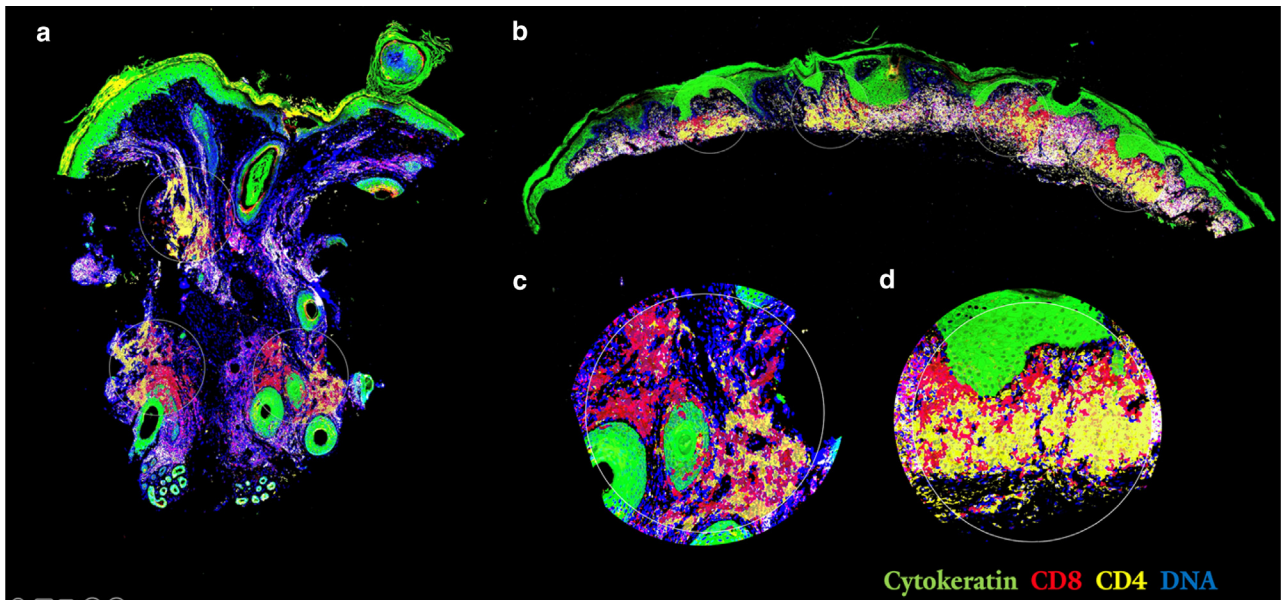


**Figure 4. Geometric ROIs from morphea tissue that failed quality control.** Not enough cells were detected in ROIs and ultimately failed quality control. Left: Note geometric ROIs in different shapes, including circles of varying sizes and polygons across spatially distinct anatomical locations. Right: Closer view of ROI #1. Morphology markers included CD45 (magenta), CD49f (green yellow), and CD90 (cyan). ROI, region of interest.

divided by uniformly spaced, equally size geometric ROIs (Figure 3). This approach is ideal for novel target discovery, particularly when morphology markers are not readily available or compartmentalized analysis is not required. For small-tissue specimens, gridded profiling may be especially useful because a grid is drawn across the entire sample, capturing cellular heterogeneity within the whole tissue. Conversely, we do not recommend the gridded approach for larger tissue sections or for tissue microarrays (TMAs). For TMAs, the gridded approach would result in the selection of regions without any tissue (ie, the space between cores). For larger tissues, this

approach would generate an excessive number of ROIs, making the experiment cost prohibitive.

**Morphology and cell-type–specific segmentation within geometric ROIs.** Perhaps the most useful profiling strategy is segmentation, which is used to divide an ROI into subdivisions or multiple segments on the basis of morphology or cell-type–specific profiling. In morphology-based segmentation, geometric ROIs are further segmented into compartments that are either positive or negative for selected visualization markers. For example, each ROI



**Figure 5. Geometric ROIs with cell-type–specific segmentation in DLE and LP.** Representative images of (a) DLE and (b) LP stained with pan-cytokeratin (green), CD8 (red), CD4 (yellow), and Syto83 (DNA, blue) for visualization and ROI selection. Each ROI is a geometric circle measuring 500  $\mu$ M in diameter. Within each ROI, cell-type–specific segmentation was performed. AOIs are shown in closer view for (c) DLE and (d) LP. AOIs are masked in similar colors as staining background: epidermis (green), CD8 T cells (red), and CD4 T cells (yellow). AOI, area of illumination; DLE, discoid lupus erythematosus; LP, lichen planus; ROI, region of interest.

could be divided into cytokeratin-positive epidermis, cytokeratin-negative dermis, and CD45+ immune cells. Then, each compartment could be separately sequenced, including the cells that do not stain for a morphology marker, such as cytokeratin-negative, CD45-negative cells representing stromal cells in the dermis. This tool is especially useful for TMAs, in which each tissue core is small, and the entire tissue section can be selected within a single circular geometric ROI and then further segmented into compartments. This allows one to capture all the cells in a small core of tissue.

Our preferred method for segmentation is cell-type-specific masking within geometric ROIs. The micromirror device in the GeoMx Digital Spatial Profiler instrument can mask UV light to a region as small as 10  $\mu\text{m}$ , which is about the diameter of a single cell; however, we found that cell-type profiling does not have the resolution of single-cell analysis, and oligos from adjacent cells can also be collected. Cell-type profiling can be used to evaluate the transcriptome of distinct cell populations using well-known biomarkers, including cytokeratin, CD3, CD4, CD8, and CD68. For example, we stained DLE and LP tissues with cytokeratin, CD4, and CD8 and performed cell-type-specific profiling for each of these markers (Figure 5). In this example, multiple geometric circles of 500  $\mu\text{m}$  in diameter were used for RNA profiling in DLE and LP (Figure 5a and b). Within each geometric circle, we performed cell-type-specific profiling within epidermis (cytokeratin-positive cells), CD4 T cells (CD4-positive cells), and CD8 T cells (CD8-positive cells) as a unique AOI (Figure 5c and d). Note that each AOI is pooled together in a single well for RNA sequencing. Thus, all the cells in red that are positive for CD8 T cells within a geometric circle in DLE (Figure 5c) are combined into a single well for analysis. This illustrates how DSP does not have single-cell resolution but can be cell-type specific. By analyzing CD8 T cells from different ROIs, you can compare CD8 T cells from the superficial, mid, or deep dermis. In this manner, DSP is analogous to bulk RNA sequencing from sorted cells with selective spatial context.

This profiling strategy may also be useful for rare cell populations and noncontiguous regions such as CD123 or B cell maturation antigen staining for plasmacytoid dendritic cells in DLE. These cells are often lost during tissue dissociation and digestion methods used to create single-cell suspensions. It is important to note that for rare cell populations, the oligos from similar ROIs across multiple samples may need to be pooled for efficient sequencing.

**Contour profiling.** For studies investigating the heterogeneity of biological gradients such as chemokines, contour profiling may be useful (Figure 3). This profiling method can be used for the chemokine gradients at the dermal-epidermal junction in interface dermatoses such as DLE and LP. In this example, the PanCK-positive epidermis could be set as center, and the transcriptome of each radiating, concentric band could be assessed to identify differentially expressed genes (DEGs) in the superficial, mid, and deep dermis. This would also capture any cells present in a manner analogous to bulk sequencing thin layers of skin. We have not yet performed contour profiling on our samples but intend to examine chemokine gradients of interface dermatoses in this manner.

Overall, we favor geometric ROIs with subsequent cell segmentation based on cell masking from morphology markers or cell-type-specific markers to allow for collection of enough transcripts from enough cells to pass QC and to assess DEGs in a cell-type-specific manner with spatial resolution (Box 2). This approach has

### Box 2. Special considerations for region-of-interest (ROI) selection and segmentation

- Select ROIs that contain at least 100 cells for efficient sequencing.
- Use at least 4–5 ROIs for a single tissue.
- A single ROI is recommended for tissue microarrays with small sample areas.
- The biological question will determine the profiling tool used.
- Recommend geometric ROIs with subsequent cell segmentation based on cell masking from morphology markers (Figure 5).

allowed us to identify unique pathways in keratinocytes and T cells in cutaneous lupus, LP, and hidradenitis suppurativa.

### Collection plate, library preparation and PCR, and NGS

After ROI and AOI selection, oligos are cleaved, and aspirates are collected into a 96-well collection plate. This is the final step of the protocol completed on the GeoMx instrument. If the samples are processed immediately, the collection plate may be sealed with a permeable membrane; however, for longer-term storage, the plate must be sealed with an adhesive foil to prevent contamination. If the plate is stored for 24 hours or less, it may be stored at 4 °C. If the plate is stored between 24 hours and 30 days, it must be stored at –20 °C. If stored for longer than 30 days, the plate must be stored at –80 °C. We recommend processing as soon as possible to prevent degradation of oligos and reduce the chance of contamination. Prior to library preparation, the collection plate is dried down and rehydrated. It is easy to introduce contamination or expose the oligos to RNase during these steps; thus, it is critical to perform these steps carefully on RNase-free surfaces.

Before library preparation, the collection plate must be dried down by incubating on a thermocycler at 65 °C for 1 hour. If plates were stored at –20 °C or –80 °C, the plastic or foil membranes must be replaced with permeable ones to allow evaporation to occur. It is important to prevent sample loss and avoid contamination during membrane replacement. Thaw the collection plates on ice and then spin plates down at 1500g for 5 minutes at 4 °C to ensure that all the oligos are in the bottom of the well. Spray all surfaces down with RNase AWAY and gently remove the adhesive foil and then replace the foil with a permeable membrane sicker. After dry down, please check that there is no liquid remaining in the plate wells. It is important that there is no liquid remaining prior to rehydrating the samples during library preparation. If there is any liquid remaining, incubate the plate for an additional 30 minutes.

In addition to collection plates (DSP plate), Nanostring provides a GeoMx Seq Code Pack Plate, a 96-well plate that contains unique dual-index barcodes required for the Illumina sequencing sample sheet. Essentially, the barcodes in the SeqCode Pack Plate helps track the ROI/AOI from which your samples were collected. For library preparation, a new PCR plate is prepared by combining GeoMx Seq Code PCR Master Mix, the primers in the Seq Code Pack, and the samples in the DSP plate. It is critical that during this step, all 3 plates—Seq Code pack, DSP collection plate, and PCR plate—are all in the correct orientation. The primers in A1 from the Seq Code Pack must be added to samples in A1 of the DSP plate, and finally, both

the samples and primers are transferred together to A1 of the new PCR plate. This step is essential for retaining the spatial information of your RNA sample. For the remaining steps, follow Nanostring's detailed guidelines, which include instructions on assessing library quality and quantity and on setting up the sequencing on Illumina sequencing platforms.

Because we do not have our own sequencing instrument, we submit our samples to a sequencing center for library preparation and NGS. Along with the DSP collection plates, we submit Seq Code Pack plates, the GeoMx Seq Code PCR Master Mix, and 3 input files that are downloaded from the GeoMx Digital Spatial Profiler. These files are the Lab worksheet, Seq Code UDI Indices, and Pipeline Config File. These files can be downloaded from the DSP platform at the completion of sample collection and are essential for setting up the Illumina NGS experiment. From sample submission to receipt of FASTQ files, it can take 2–4 weeks. Once FASTQ files are received, they need to be transferred and processed by Nanostring's GeoMx NGS Pipeline software program to converted to DCC files. The DCC files can be uploaded back to the GeoMx Digital Spatial Profiler system for data analysis (Box 3).

### Data analysis

**Data analysis: QC.** When analyzing spatial data using GeoMx Digital Spatial Profiler, several key steps are taken to ensure the quality and reliability of the results (Box 4). To perform QC, segment QC and biological probe QC should be run in the GeoMx software. Segment QC is the initial step, and it evaluates the quality of sequencing for each segment. It examines technical signal, technical background noise, and DSP parameters, such as the minimum number of nuclei and surface area count. These parameters help in assessing whether the data meet the expected quality standards. It is recommended to use default settings for technical signal and technical background QC. However, DSP parameters can be adjusted on the basis of tissue type and selected ROI size. We typically use minimum detection of at least 20 estimated nuclei and 1000 transcript reads probe counts per ROI. However, in practice, we try to ensure that at least 100 nucleated cells are present in each ROI to avoid failure. Unfortunately, sparsely infiltrated tissues may fail this QC step as was the case with our morphea tissue (Figure 4).

### Box 3. Special considerations for sample collection, library preparation, and next-generation sequencing (NGS)

- Store collection plate at 4 °C is performing library preparation and NGS within 48 hours. Store at –20 °C if used within 30 days and –80 °C if longer.
- Prevent contamination during membrane exchanges and drying steps.
- Make sure that the collection plate, Seq Code Pack Plate, and PCR plate are all in the proper orientation during library preparation.
- Download the Lab Worksheet, Seq Code UDI Indices, and Pipeline Confit file and submit them to the sequencing center.

### Box 4. Special considerations for data analysis

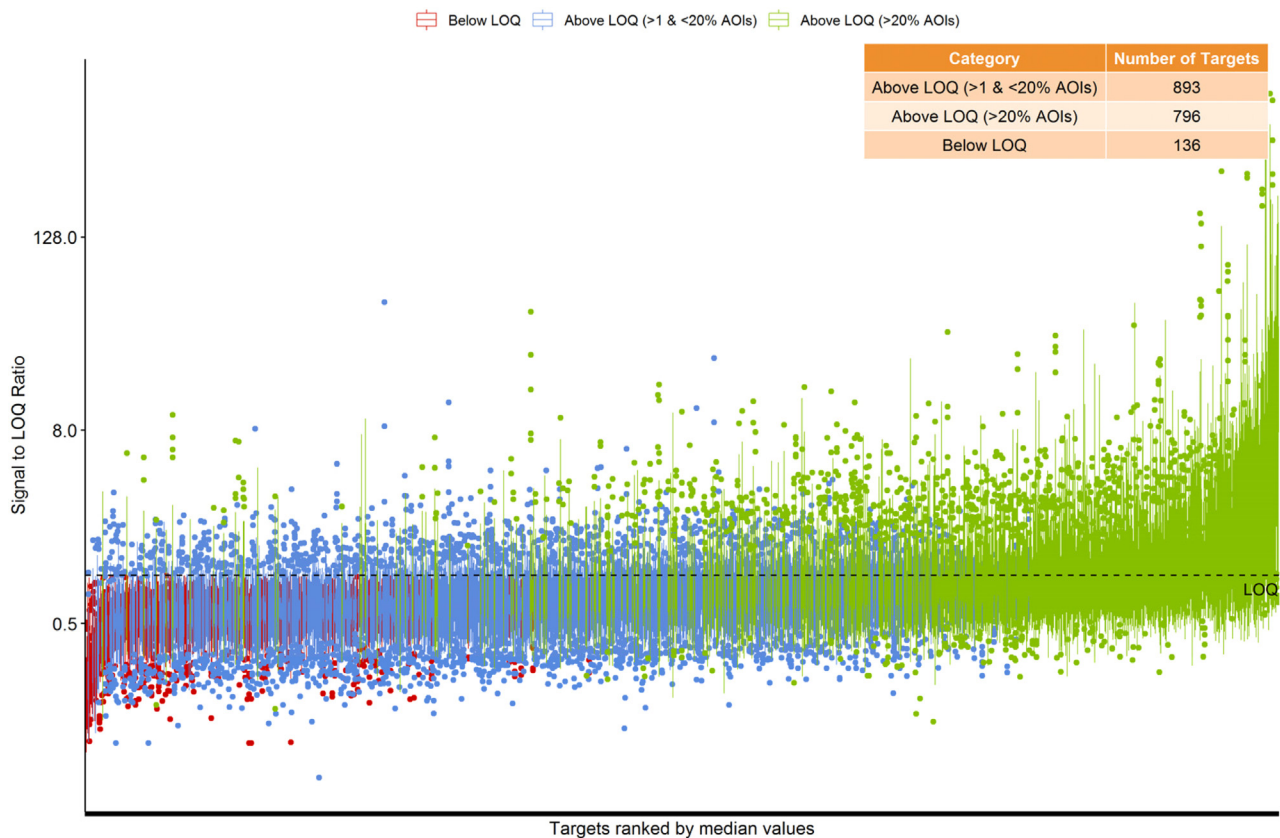
- Ensure at least 20 nucleated for each ROI/area of illumination (AOI) when performing technical quality control.
- Q3 normalization should be used when analyzing large probe sets.
- Linear mixed model for multiple ROIs/AOIs per sample.
- Use multiple *t*-tests with Benjamini–Hochberg procedure (false discovery rate).
- May need to export data from instrument to generate figures and additional bioinformatics.

In biological probe QC, the focus shifts to the assessment of individual probes within the dataset. The aim is to identify and exclude outlier probes that may skew the results. For RNA assays, this includes detecting dropout probes and setting a limit of quantitation (LOQ) as a confidence threshold. In protein assays, the focus is primarily on setting the LOQ. Probes designated with a warning status are flagged for reference.

After QC checks, the next crucial step for optimal data analysis is choosing the right normalization method. Traditional methods such as housekeeping gene normalization work well when experimental conditions are uniform, precise, and homogeneous, such as when studying a single cell type. For example, if only the normalization of the CD8a+ compartment is needed, then housekeeping gene normalization can be performed, but if normalization of all compartments simultaneously is required, then Q3 normalization is recommended. This is because in high-plex data and heterogeneous samples, such as those found in complex tissues or diseased states, housekeeping gene normalization may not be sufficient. Q3 normalization adjusts gene expression data to ensure similar expression ranges across all compartments, regardless of their size or composition. It is particularly useful when analyzing large and diverse probe panels targeting the full transcriptome. However, it may not be suitable for smaller, targeted panels or when segments have low signal above background. Using both Q3 and housekeeping gene normalization methods in parallel can provide researchers with a robust approach to ensure the reliability of their findings, especially when dealing with diverse and complex biological samples. We used Q3 normalization for our study using RNA CTA assay on DLE, LP, and psoriasis tissues (Figure 2). Across all ROIs, 1689 of 1825 genes pass Q3 normalization using LOQ (Figure 6). The remaining 1689 genes are then used for statistical tests and data visualization to be discussed below.

**Data analysis: statistical tests and data visualization.** After QC and data normalization, statistical tests and data visualization may be performed using the GeoMx Digital Spatial Profiler Analysis suite on the instrument. Because multiple ROIs/AOIs can come from the same individual sample, a linear mixed model (LMM) is to generate data for individual sample. Then, differential gene expression can be performed at the level of individual samples in addition to additional ROIs/AOIs. The resulting *P*-values are adjusted for multiple comparisons with the Benjamini–Hochberg procedure (false discovery rate [FDR]). Data may be visualized on the instrument with





**Figure 6. Cancer Transcriptome Atlas LOQ after Q3 normalization.** (a) Signal to LOQ ratio for RNA counts in Cancer Transcriptome Atlas using signal of detected RNA probes divided by the geometric mean of 8 negative probes. Only genes with signal above LOQ were included in analysis (1689 genes of 1825). LOQ, limit of quantification.

heatmaps, volcano plots, box plots, or scatter plots. Often, we download data and generate figures with third-party platforms such as GraphPad Prism.

To illustrate the type of data generated, we briefly discuss a small pilot experiment using the RNA CTA assay on samples of DLE, LP, and psoriasis. The emphasis is on the type of data generated rather than the biological implications of this illustrative study. Three samples of DLE, LP, and psoriasis and normal skin were initially stained with morphological markers CD3e, CD8a, and PanCK to identify ROIs (Figure 2). An LMM was used to detect DEGs with an FDR <0.05 using Benjamini–Hochberg correction. Next, we compared DEGs between DLE and control tissues within the T-cell–enriched ROIs (Figure 7a) and PanCK+ epidermis (Figure 7b) as visualized by volcano plots. T-cell–enriched areas of DLE showed increased expression of chemokines, cytokines, IFN signaling, and antigen processing and presentation. DLE epidermis also expressed IFN-related genes, antigen processing and presentation, and keratinocyte growth compared with normal epidermis. Unique DEGs were also identified for LP compared with those for controls (Figure 7c and d) for and psoriasis compared with those for controls (Figure 7e and f). Importantly, known pathogenic cytokines for psoriasis such as *IL17A*, *IL17F*, and *IL23* are not included in the CTA RNA panel, highlighting the importance of choosing the proper RNA probe set.

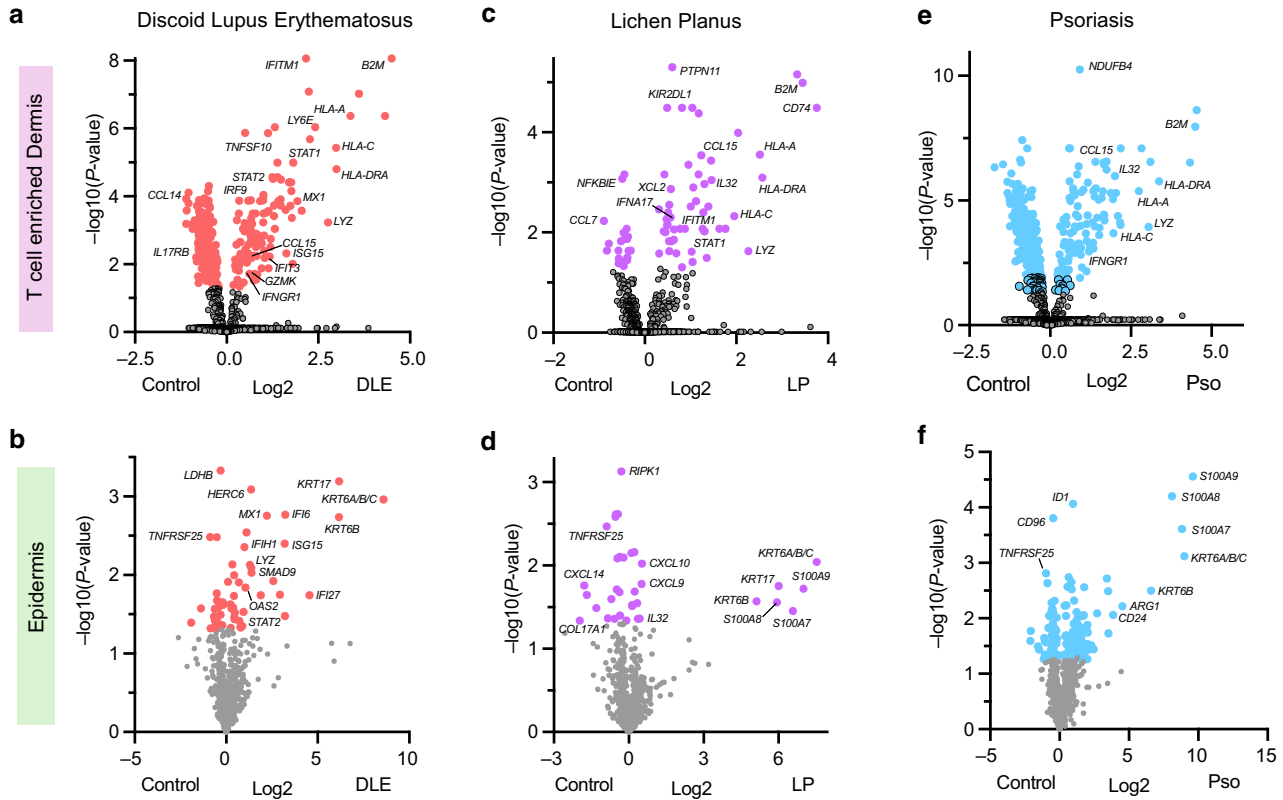
We next directly compared samples of DLE, psoriasis, and LP with one another. DEGs were identified in T-cell–rich areas as well as the epidermis across disease comparisons (Figure 8). The epidermis between DLE and LP was very similar, suggesting a shared

inflammatory reaction pattern of interface dermatoses, at least by the CTA assay (Figure 8b). There are several limitations to this pilot study, and our objective is to illustrate data output from DSP rather than provide new biologic insights. Any conclusions are significantly limited by the small cohort of patients. As such, our goal is a preliminary demonstration of how DSP can generate novel insights into inflammatory pathway activation in inflammatory skin diseases such as psoriasis, LP, and DLE. Despite these limitations and small sample size, DSP was able to confirm findings of multiple previous studies (Domingues et al, 2015; Hussein et al, 2008; Shao et al, 2019; Stannard et al, 2017; Thorpe et al, 2014; Wenzel et al, 2009).

#### DISCUSSION AND POTENTIAL APPLICATIONS

In this section, we provide an overview of DSP as an application to detect genes within intact tissues such as skin. In addition, we offered our experience in the technical and practical use of DSP on inflammatory skin diseases. In this manner, we demonstrate the potential utility of DSP to profile autoimmune skin diseases with distinct inflammatory histological patterns. Ultimately, our objective is to demonstrate to investigators how this method could be used for their studies and provide insight that is not available in the manufacturer’s guidelines.

One advantage of in situ–based transcriptomic approaches is profiling unique immune subsets that are difficult to isolate from the skin and are often lost during tissue processing for scRNA-seq. DSP offers flexibility to perform both exploratory



**Figure 7. Differential gene expression of DLE, LP, and psoriasis compared with those of controls using Cancer Transcriptomic Atlas RNA panel.** (a, b) Volcano plot comparing CD3/CD8-enriched ROIs in (a) dermis and PanCK-positive ROI in (b) epidermis of DLE and healthy controls with Cancer Transcriptome Atlas RNA panel. (c, d) Volcano plot comparing CD3/CD8-enriched ROIs in (c) dermis and PanCK-positive ROI in (d) epidermis of LP and healthy controls. (e, f) Volcano plot comparing CD3/CD8-enriched ROIs in (e) dermis and PanCK-positive ROI in (f) epidermis of psoriasis and healthy controls. Significant genes are colored (FDR < 0.05). DLE, discoid lupus erythematosus; FDR, false discovery rate; LP, lichen planus; PanCK, pan-cytokeratin; ROI, region of interest.

and hypothesis-generating experiments with WTA and CTA as well as customized panels to interrogate specific pathways in tissues.

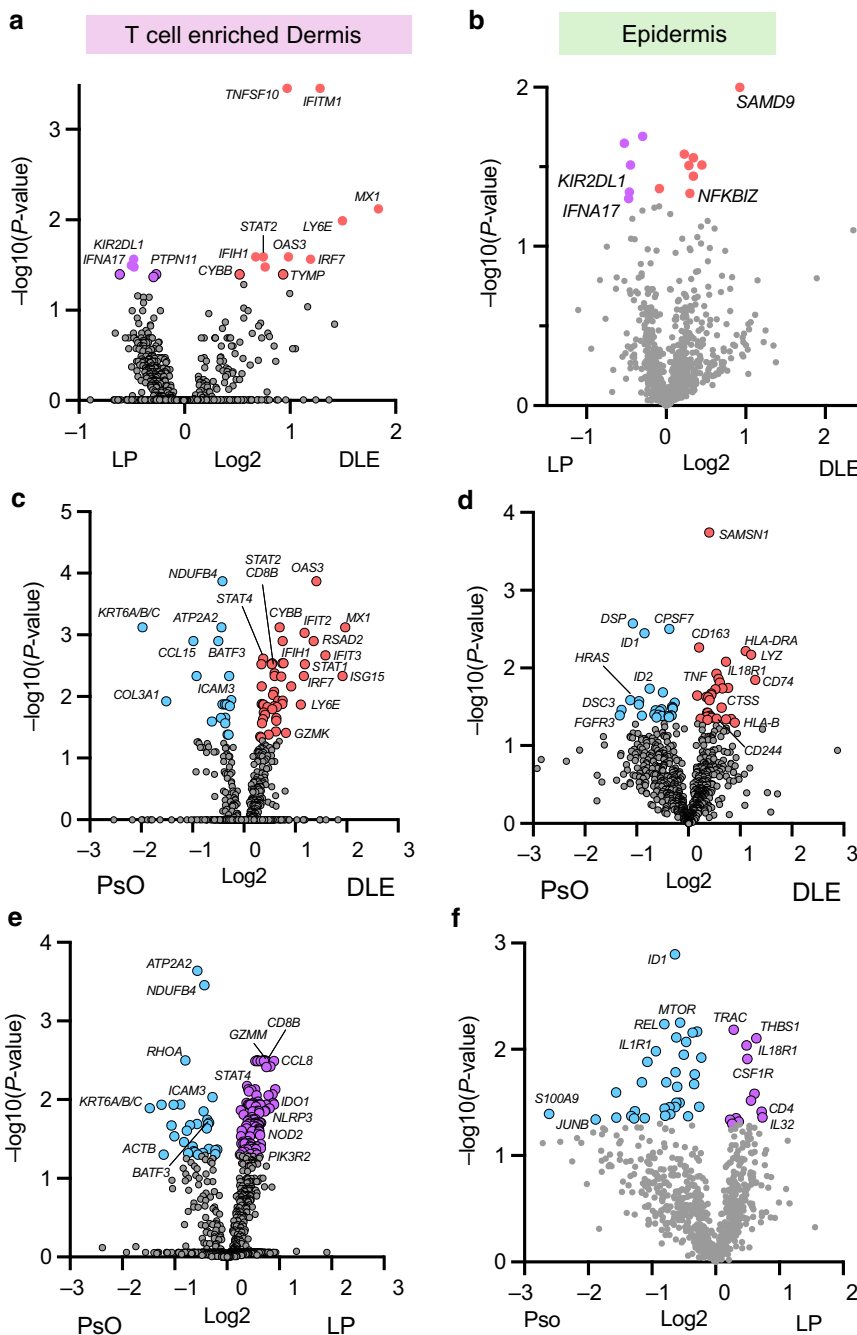
One limitation to tissue-based protein or gene expression profiling is the lack of high-throughput approaches due to space constraints of how much tissue can fit on a single slide. A possible solution is the generation of TMAs, where cores of tissue are removed from dozens of individual specimens and collated into a new paraffin-embedded block. This approach has widely been used to study the immune infiltrate of cancers. This may be appropriate for diseases such as LP where the inflammation is continuous and relatively homogenous at the dermal–epidermal junction. For cutaneous lupus samples, multiple cores of tissues would be needed to sample distinct anatomic locations given heterogenous infiltrate.

Another potential limitation of DSP is that it is not single-cell resolution. This is also true for the Visium platform from 10x Genomics. Nevertheless, critical insights into inflammatory skin diseases can still be uncovered with these non–single-cell approaches (Billi et al, 2022; Brumfiel et al, 2022; Castillo et al, 2023; Macchiarella et al, 2023). Recently, true single-cell spatial transcriptomic profiling platforms are available, including Nanostring CosMx Spatial Molecular Imager (He et al, 2022) and 10x Genomics Xenium. Both platforms detect transcripts at subcellular resolution. Currently, both platforms offer gene profiling up to 6000 genes. In the next year or 2, whole-transcriptome single-

cell imaging will be available from both platforms. Curio Biosciences has developed Curio Seeker, which uses 10-mm spatially indexed beads for subcellular resolution. However, in our experience, Curio Seeker performs poorly on skin samples, and we do not recommend it for studying inflammatory skin diseases. Other platforms also exist such as multiplex error-robust FISH by Vizgen that achieves near genome-wide, single-cell spatial profiling that may be useful for studying inflammatory skin diseases. Integration of data from scRNA-seq and spatial transcriptomics that do not have single-cell resolution is a powerful strategy to overcome the current limitations (Houser et al, 2023; Thrane et al, 2023).

### CONCLUSION

In summary, DSP is one current spatial transcriptomic platform being used to decipher insights into disease pathogenesis that has predominately been used for cancer and is now more frequently being used in inflammatory skin diseases. There are several unique features of DSP, including multi-modal detection of RNA and proteins, use of immunofluorescent probes to define morphology markers prior to profiling RNA or proteins, use of ROIs and segmentation tools rather than gridded barcoding slides, and no special slides needed for tissue placement. In our experience, DSP will remain an invaluable tool to perform spatial transcriptomics and spatial proteomics in inflammatory skin diseases. In this paper, we have provided a technical and practical guide for



**Figure 8. Differential gene expression between DLE, LP, and PsO using Cancer Transcriptomic Atlas RNA panel.** (a, b) Volcano plot comparing CD3/CD8-enriched ROIs in (a) dermis and PanCK-positive ROI in (b) epidermis of LP and DLE. (c, d) Volcano plot comparing CD3/CD8-enriched ROIs in (c) dermis and PanCK-positive ROI in (d) epidermis of PsO and DLE. (e, f) Volcano plot comparing CD3/CD8-enriched ROIs in (e) dermis and PanCK-positive ROI in (f) epidermis of LP and PsO. Significant genes are colored (FDR < 0.05). DLE, discoid lupus erythematosus; FDR, false discovery rate; LP, lichen planus; PanCK, pan-cytokeratin; PsO, psoriasis; ROI, region of interest.

performing DSP, including potential pitfalls, tips for optimal workflow, and statistical considerations. The methods described in this paper are not a summary of the manufacturer's guidelines but rather a user's perspective on best practices and user-friendly approaches found outside the protocols.

## MATERIALS AND METHODS

### Human tissues

Samples of DLE (n = 3), LP (n = 3), psoriasis (n = 3), and control skin from cyst excisions (n = 3) from archived FFPE tissue were obtained from Yale Dermatopathology biorepository (Table 1). Staining of archived human FFPE tissue was approved by Yale Institutional

Review Board (Human Investigative Committee number 15010105235). Clinical characteristics were provided after tissue analysis on blinded, archived biospecimens.

### Antibodies for IF

For the fluorescent markers, we used Syto83 at 500  $\mu$ M for nuclei visualization: CD3-AF594 (Novus Biological, C3e/1308, 1:100), CD8-647 (Novus Biological, SPM548, 1:200), and PanCK-AF488 (Novus Biological, AE1/AE3, 1:500).

### Statistical analysis

For CTA, an LMM or unpaired *t*-test was used for analysis, with the resulting *P*-values adjusted for multiple comparisons with the Benjamini–Hochberg procedure (FDR) and considering the size of



ROIs and slide scanning batch effect. *P*-value or FDR < 0.05 were considered significant, with *P* < .01 considered highly significant.

#### ETHICS STATEMENT

Staining of archived human formalin-fixed, paraffin-embedded tissue was approved by Yale University Institutional Review Board (Human Investigative Committee number 15010105235). Clinical characteristics were provided after tissue analysis on anonymized, archived biospecimens.

#### DATA AVAILABILITY STATEMENT

List of targeted genes within Cancer Transcriptomic Atlas and primary data are available on Mendeley. Datasets related to this article can be found at <https://data.mendeley.com/datasets/bv5rph7w9h/1> hosted by Mendeley.

#### ORCID

Christina Cho: <http://orcid.org/0000-0001-5482-9533>  
 Nazgol-Sadat Haddadi: <http://orcid.org/0000-0001-8854-8182>  
 Michal Kidacki: <http://orcid.org/0000-0002-3279-5974>  
 Gavitt A. Woodard: <http://orcid.org/0000-0003-1985-9598>  
 Saeed Shakiba: <http://orcid.org/0000-0002-0942-9351>  
 Ümmügülsüm Yıldız-Altay: <http://orcid.org/0000-0001-8774-9257>  
 Jillian M. Richmond: <http://orcid.org/0000-0003-1589-6770>  
 Matthew D. Vesely: <http://orcid.org/0000-0001-9363-945X>

#### CONFLICT OF INTEREST

Spouse of MDV is an employee at Regeneron Pharmaceuticals. JMR is an inventor on patent application #15/851,651 and on patent #63489191. The remaining authors state no conflict of interest.

#### DECLARATION OF GENERATIVE ARTIFICIAL INTELLIGENCE (AI) OR LARGE LANGUAGE MODELS (LLMs)

The author(s) did not use AI/LLM in any part of the research process and/or manuscript preparation.

#### ACKNOWLEDGMENTS

We thank the pathologists and staff of Yale Dermatopathology for their assistance, especially Dilgash Mekael, Emily Hast, William Damsky, and Jennifer M. McNiff. Funding for this project was through KL2 TR001862 from National Center for Advancing Translational Sciences to MDV. MDV is supported by National Institute of Arthritis and Musculoskeletal and Skin Diseases of the National Institutes of Health under award number K08AR080777. JMR is supported by a Target Identification in Lupus Award from the Lupus Research Alliance.

#### AUTHOR CONTRIBUTIONS

Conceptualization: CC, JMR, MDV; Data Curation: MDV, JMR; Formal Analysis: CC, MDV; Funding Acquisition: MDV; Resources: MDV; Supervision: JMR, MDV; Visualization: CC, MDV; Writing – Original Draft Preparation: CC, N-SH, MK, GAW, JMR, MDV; Writing – Review and Editing: CC, NS-H, MK, GAW, SS, ÜY-A, JMR, MDV

#### REFERENCES

Baena-Del Valle JA, Zheng Q, Hicks JL, Fedor H, Trock BJ, Morrissey C, et al. Rapid loss of RNA detection by in situ hybridization in stored tissue blocks and preservation by cold storage of unstained slides. *Am J Clin Pathol* 2017;148:398–415.

Billi AC, Ma F, Plazyo O, Gharaee-Kermani M, Wasikowski R, Hile GA, et al. Nonlesional lupus skin contributes to inflammatory education of myeloid cells and primes for cutaneous inflammation. *Sci Transl Med* 2022;14:eabn2263.

Brumfiel CM, Patel MH, Severson KJ, Zhang N, Li X, Quillen JK, et al. Ruxolitinib cream in the treatment of cutaneous Lichen Planus: a prospective, open-label study. *J Invest Dermatol* 2022;142:2109–2116.e4.

Cabrita R, Lauss M, Sanna A, Donia M, Skaarup Larsen M, Mitra S, et al. Tertiary lymphoid structures improve immunotherapy and survival in melanoma. *Nature* 2020;577:561–5.

Castillo RL, Sidhu I, Dolgalev I, Chu T, Prystupa A, Subudhi I, et al. Spatial transcriptomics stratifies psoriatic disease severity by emergent cellular ecosystems. *Sci Immunol* 2023;8:eabq7991.

Domingues R, de Carvalho GC, da Silva Oliveira LM, Futata Taniguchi E, Zimbres JM, Aoki V, et al. The dysfunctional innate immune response

triggered by toll-like receptor activation is restored by TLR7/TLR8 and TLR9 ligands in cutaneous lichen planus. *Br J Dermatol* 2015;172:48–55.

Emmert-Buck MR, Bonner RF, Smith PD, Chuaqui RF, Zhuang Z, Goldstein SR, et al. Laser capture microdissection. *Science* 1996;274:998–1001.

Gartrell-Corrado RD, Chen AX, Rizk EM, Marks DK, Bogardus MH, Hart TD, et al. Linking transcriptomic and imaging data defines features of a favorable tumor immune microenvironment and identifies a combination biomarker for primary MelanomaTranscriptomic. *Cancer Res* 2020;80:1078–87.

He S, Bhatt R, Brown C, Brown EA, Buhr DL, Chantranuvatana K, et al. High-plex imaging of RNA and proteins at subcellular resolution in fixed tissue by spatial molecular imaging. *Nat Biotechnol* 2022;40:1794–806.

Helmink BA, Reddy SM, Gao J, Zhang S, Basar R, Thakur R, et al. B cells and tertiary lymphoid structures promote immunotherapy response. *Nature* 2020;577:549–55.

Houser AE, Kazmi A, Nair AK, Ji AL. The use of single-cell RNA-sequencing and spatial transcriptomics in understanding the pathogenesis and treatment of skin diseases. *JID Innov* 2023;3:100198.

Hussein MRA, Aboulhagag NM, Atta HS, Atta SM. Evaluation of the profile of the immune cell infiltrate in lichen planus, discoid lupus erythematosus, and chronic dermatitis. *Pathology* 2008;40:682–93.

Kiuru M, Kriner MA, Wong S, Zhu G, Terrell JR, Li Q, et al. High-plex spatial RNA profiling reveals cell type-specific biomarker expression during melanoma development. *J Invest Dermatol* 2022;142:1401–1412.e20.

Langer-Safer PR, Levine M, Ward DC. Immunological method for mapping genes on *Drosophila* polytene chromosomes. *Proc Natl Acad Sci USA* 1982;79:4381–5.

Macchiarella G, Cornacchione V, Cojean C, Riker J, Wang Y, Te H, et al. Disease association of anti-carboxyethyl lysine autoantibodies in hidradenitis suppurativa. *J Invest Dermatol* 2023;143:273–283.e12.

Meier-Ruge W, Bielser W, Remy E, Hillenkamp F, Nitsche R, Unsöld R. The laser in the Lowry technique for microdissection of freeze-dried tissue slices. *Histochem J* 1976;8:387–401.

Merritt CR, Ong GT, Church SE, Barker K, Danaher P, Geiss G, et al. Multiplex digital spatial profiling of proteins and RNA in fixed tissue. *Nat Biotechnol* 2020;38:586–99.

Piñeiro AJ, Houser AE, Ji AL. Research techniques made simple: spatial transcriptomics. *J Invest Dermatol* 2022;142:993–1001.e1.

Rozeman EA, Prevoov W, Meier MAJ, Sikorska K, Van TM, van de Wiel BA, et al. Phase Ib/II trial testing combined radiofrequency ablation and ipilimumab in uveal melanoma (SECIRA-UM). *Melanoma Res* 2020;30:252–60.

Rudkin GT, Stollar BD. High resolution detection of DNA–RNA hybrids in situ by indirect immunofluorescence. *Nature* 1977;265:472–3.

Scatena C, Murtas D, Tomei S. Cutaneous melanoma classification: the importance of high-throughput genomic technologies. *Front Oncol* 2021;11:635488.

Schäbitz A, Hillig C, Mubarak M, Jargosch M, Farnoud A, Scala E, et al. Spatial transcriptomics landscape of lesions from non-communicable inflammatory skin diseases. *Nat Commun* 2022;13:7729.

Shao S, Tsoi LC, Sarkar MK, Xing X, Xue K, Uppala R, et al. IFN-gamma enhances cell-mediated cytotoxicity against keratinocytes via JAK2/STAT1 in lichen planus. *Sci Transl Med* 2019;11:eaav7561.

Stannard JN, Reed TJ, Myers E, Lowe L, Sarkar MK, Xing X, et al. Lupus skin is primed for IL-6 inflammatory responses through a keratinocyte-mediated autocrine Type I interferon loop. *J Invest Dermatol* 2017;137:115–22.

Theocharidis G, Thomas BE, Sarkar D, Mumme HL, Pilcher WJR, Dwivedi B, et al. Single cell transcriptomic landscape of diabetic foot ulcers. *Nat Commun* 2022;13:181.

Thorpe RB, Gray A, Kumar KR, Susa JS, Chong BF. Site-specific analysis of inflammatory markers in discoid lupus erythematosus skin. *ScientificWorldJournal* 2014;2014:925805.

Thrane K, Winge MCG, Wang H, Chen L, Guo MG, Andersson A, et al. Single-cell and spatial transcriptomic analysis of human skin delineates intercellular communication and pathogenic cells. *J Invest Dermatol* 2023;143:2177–2192.e13.

- Toki MI, Merritt CR, Wong PF, Smithy JW, Kluger HM, Syrigos KN, et al. High-plex predictive marker discovery for melanoma immunotherapy-treated patients using digital spatial ProfilingHigh-Plex discovery with digital spatial profiling. *Clin Cancer Res* 2019;25:5503–12.
- Van Herck Y, Antoranz A, Andhari MD, Milli G, Bechter O, De Smet F, et al. Multiplexed immunohistochemistry and digital pathology as the foundation for next-generation pathology in melanoma: methodological comparison and future clinical applications. *Front Oncol* 2021;11:636681.
- Van TM, Blank CU. A user's perspective on GeoMx™ digital spatial profiling. *Immuno-oncol Technol* 2019;1:11–8.
- Vathiotis IA, Yang Z, Reeves J, Toki M, Aung TN, Wong PF, et al. Models that combine transcriptomic with spatial protein information exceed the predictive value for either single modality. *NPJ Precis Oncol* 2021;5:45.
- Veenstra J, Dimitrion P, Yao Y, Zhou L, Ozog D, Mi QS. Research techniques made simple: use of imaging mass cytometry for dermatological research and clinical applications. *J Invest Dermatol* 2021;141:705–712.e1.
- Vesely M, Martinez-Morilla S, Gehlhausen JR, McNiff JM, Whang PG, Rimm D, et al. Not all well-differentiated cutaneous squamous cell carcinomas are equal: tumors with disparate biologic behavior have differences in protein expression via digital spatial profiling. *J Am Acad Dermatol* 2022;87:695–8.
- Wenzel J, Zahn S, Bieber T, Tüting T. Type I interferon-associated cytotoxic inflammation in cutaneous lupus erythematosus. *Arch Dermatol Res* 2009;301:83–6.
- Whitley SK, Li M, Kashem SW, Hirai T, Igyártó BZ, Knizner K, et al. Local IL-23 is required for proliferation and retention of skin-resident memory TH17 cells. *Sci Immunol* 2022;7:eabq3254.



**This work is licensed under a Creative Commons Attribution-NonCommercial-NoDerivatives 4.0 International License. To view a copy of this license, visit <http://creativecommons.org/licenses/by-nc-nd/4.0/>**